

# Contrasting origins of Cenozoic silicic volcanic rocks from the western Cordillera of the United States

Eric H. Christiansen · Michael McCurry

Received: 1 September 2005 / Accepted: 8 February 2007 / Published online: 20 June 2007  
© Springer-Verlag 2007

**Abstract** Two fundamentally different types of silicic volcanic rocks formed during the Cenozoic of the western Cordillera of the United States. Large volumes of dacite and rhyolite, mostly ignimbrites, erupted in the Oligocene in what is now the Great Basin and contrast with rhyolites erupted along the Snake River Plain during the Late Cenozoic. The Great Basin dacites and rhyolites are generally calc-alkaline, magnesian, oxidized, wet, cool (<850°C), Sr- and Al-rich, and Fe-poor. These silicic rocks are interpreted to have been derived from mafic parent magmas generated by dehydration of oceanic lithosphere and melting in the mantle wedge above a subduction zone. Plagioclase fractionation was minimized by the high water fugacity and oxide precipitation was enhanced by high oxygen fugacity. This resulted in the formation of Si-, Al-, and Sr-rich differentiates with low Fe/Mg ratios, relatively

low temperatures, and declining densities. Magma mixing, large proportions of crustal assimilation, and polybaric crystal fractionation were all important processes in generating this Oligocene suite. In contrast, most of the rhyolites of the Snake River Plain are alkaline to calc-alkaline, ferroan, reduced, dry, hot (830–1,050°C), Sr- and Al-poor, and Nb- and Fe-rich. They are part of a distinctly bimodal sequence with tholeiitic basalt. These characteristics were largely imposed by their derivation from parental basalt (with low  $f_{\text{H}_2\text{O}}$  and low  $f_{\text{O}_2}$ ) which formed by partial melting in or above a mantle plume. The differences in intensive parameters caused early precipitation of plagioclase and retarded crystallization of Fe–Ti oxides. Fractionation led to higher density magmas and mid-crustal entrapment. Renewed intrusion of mafic magma caused partial melting of the intrusive complex. Varying degrees of partial melting, fractionation, and minor assimilation of older crust led to the array of rhyolite compositions. Only very small volumes of distinctive rhyolite were derived by fractional crystallization of Fe-rich intermediate magmas like those of the Craters of the Moon–Cedar Butte trend.

---

This paper constitutes part of a special issue dedicated to Bill Bonnichsen on the petrogenesis and volcanology of anorogenic rhyolites.

---

Editorial responsibility: W Leeman

---

**Electronic supplementary material** The online version of this article (doi:10.1007/s00445-007-0138-1) contains supplementary material, which is available to authorized users.

---

E. H. Christiansen (✉)  
Department of Geological Sciences, Brigham Young University,  
Provo, UT 84602, USA  
e-mail: eric\_christiansen@byu.edu

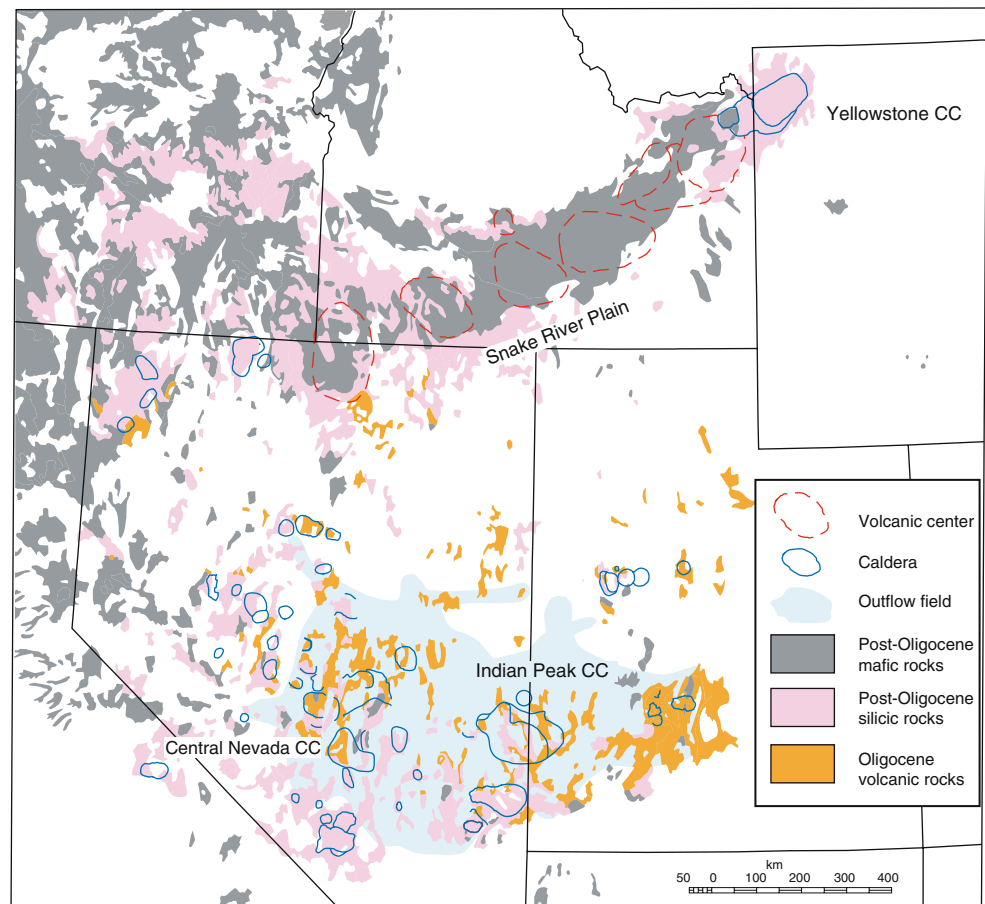
M. McCurry  
Department of Geosciences, Idaho State University,  
Pocatello, ID 83209, USA  
e-mail: mccumich@isu.edu

**Keywords** Snake River Plain · Great Basin · Ignimbrite · Rhyolite · A-type · Subduction · Dacite

## Introduction

The origin of silicic magma remains a fundamental problem. This is especially the case for rhyolites found in “anorogenic” settings—here taken to be continental rifts and hotspots. In order to better understand the origin of these rocks in general and to elucidate the origin of Snake River Plain rhyolites in particular, we contrast their

**Fig. 1** Simplified geologic map of the western United States showing the location of Oligocene and younger volcanic rocks (after King and Biekman 1974). Extent of outflow sheets are shown for the Oligocene Central Nevada and Indian Peak caldera complexes and for the younger, Yellowstone-related calderas. After Pierce and Morgan (1992), Chuang et al. (2003) and MG Best and SC Grommé (written communication 2005)



compositions with silicic volcanic rocks erupted during the middle Cenozoic of the Great Basin.

During the Oligocene, a large “ignimbrite flareup” peaked in what is now the Great Basin of Nevada and western Utah (Fig. 1) with dacite and rhyolite dominant (Best and Christiansen 1991). During the Late Cenozoic, rhyolite lavas and ignimbrites erupted along the Snake River Plain (Fig. 1). The Yellowstone caldera is the youngest example of these silicic magmatic systems (Christiansen 2001).

Below we summarize the characteristics of these large volume silicic magmas and their more mafic contemporaries. The differences between these suites suggest that the Oligocene dacites and rhyolites of the Great Basin were the result of continuous differentiation and complex mixing and crustal assimilation processes involving mafic parents that were wet, oxidized, and enriched in water-soluble trace elements—all strong links to their subduction zone heritage. In contrast, anorogenic (A-type or within-plate) rhyolites of the Snake River Plain formed dominantly by partial melting of recent crustal additions of basalt related to a mantle plume. The rhyolite sources were thus isotopically unevolved, enriched in Nb and high field strength elements, with low  $f\text{H}_2\text{O}$ , and reduced compared to the parents of the subduction-related Oligocene suite.

## Database

Data for this study were compiled from the literature, from unpublished theses, open-file reports in the state and federal geological surveys, and from our own unpublished analyses. The database contains partial chemical or isotopic data for nearly 1,900 samples from the Snake River Plain and about 1,000 samples from the Indian Peak and Central Nevada caldera complexes. The complete reference list is available in the Electronic Supplementary Material.

## Volcanology and emplacement

The Oligocene volcanic fields of the southern Great Basin are essentially centered on two large caldera complexes (Fig. 1). The Indian Peak complex contains four mapped calderas evidenced by thick intracaldera tuff sequences and collapse breccias. Two other calderas are inferred by the presence of large ash-flow sheets. The three large dacitic ignimbrites considered here had volumes of at least 1,500–3,000 km<sup>3</sup> (Best et al. 1989). Rhyolite ignimbrites are smaller in volume (each less than a few hundred km<sup>3</sup>) and are mostly caldera fill deposits. Silicic lava flows are

present locally in small volumes. Volcanism started about 34 Ma, peaked about 30 Ma and persisted into the Miocene when bimodal volcanism developed (Best et al. 1989). The Neogene lavas and tuffs are not considered here. The Central Nevada caldera complex is larger and includes at least a dozen calderas. Although the largest sheets are still dacitic, there are multiple sheets of rhyolite tuff with larger volumes than those in the Indian Peak volcanic field. Small volumes of intermediate composition lavas erupted on the flanks of both caldera complexes and locally within them. Composite volcanoes were of trivial extent in both volcanic fields. Best and Christiansen (1991) and Best et al. (1989) concluded that the magmatism was caused by dehydration of a subducting slab of oceanic lithosphere and melting in the overlying mantle. This produced wet, oxidized mafic magmas that rose, hybridized, mixed, and fractionated in the overthickened continental crust.

The Neogene magmatism along the Snake River Plain is dominated by the eruption of large volumes of rhyolite (Leeman 1982; Smith 2004). Well-studied individual ignimbrite sheets are as large as a few 1,000 km<sup>3</sup>. Lava may dominate some of the volcanic fields in the western Snake River Plain (Bonnichsen 1982). However, the easternmost volcanic fields are centered on large collapse calderas. Throughout much of the central part of the plain, the silicic rocks are buried by a few 100 m to as much as 1 km of basaltic lava flows. Burial by basalt has made it difficult to correlate ignimbrites exposed on the north with those on the south and has rendered volume estimates uncertain. Nonetheless, many outflow sheets are as much as 100 m thick and may have total volumes of thousands of cubic kilometers (Christiansen 2001). Basalt erupted mainly from small (typically less than 25 km<sup>3</sup> each) shield volcanoes (Greeley 1982), although compositionally distinctive lavas from the Craters of the Moon National Monument erupted from fissures (Leeman et al. 1976). Locally, scoria cones, tuff cones, and tuff rings are important. The rhyolites generally become younger to the northeast (Armstrong et al. 1975). Basaltic lavas do not follow this same progression; lavas less than a few thousand years old are found in the central and eastern Snake River Plain. Although the oldest surficial basalts (more than a few million years old) are concentrated in the western Snake River Plain, Champion et al. (2002) have found basaltic lavas as old as 4 Ma in drill holes in the eastern Snake River Plain.

The volcanism of Snake River Plain is typically related to the passage of the North American plate over the Yellowstone mantle plume (Morgan 1972). Christiansen et al. (2002) have suggested that the melting anomaly is shallow and unrelated to a deep mantle plume. However, Smith (2004) and Yuan and Dueker (2005) have discovered a low seismic velocity anomaly that extends to at least 500 km deep. Seismic, gravity, and topographic data reveal a 10-km-thick body of

reflective, dense rocks starting at a depth of about 10 km below the eastern Snake River Plain (Mabey 1978; Sparlin et al. 1982; Smith and Braile 1994; Peng and Humphreys 1998). This layer is thought to be an intrusive complex composed of variably differentiated tholeiitic gabbros and is commonly called the “mid-crustal sill” though it is more likely a complex system of multiple dikes and sills.

### Petrography and mineralogy

The silicic rocks of the Indian Peak and Central Nevada caldera complexes (which we will refer to as the Great Basin volcanic fields) are varied, but the typical dacite ignimbrites are crystal-rich with as much as 50% phenocrysts. The typical assemblage is plagioclase, hornblende, biotite, quartz, magnetite, ilmenite, apatite, and zircon. Titanite, pyroxenes, or sanidine are found in some units. The rhyolites range from this mineral assemblage to plagioclase, sanidine, quartz, biotite, Fe–Ti oxides, apatite, and zircon. The mafic silicates are typically Mg-rich (Ross et al. 2002; Maughan et al. 2001; Nusbaum 1990; Nielsen 1992; Radke et al. 1992). One member of the rhyolitic Shingle Pass Formation is unusual in that it has fayalite and chevkinite (Nielsen 1992). Contemporaneous andesites typically contain two-pyroxenes and plagioclase, although hornblende and olivine occur in a few (Barr 1993).

The rhyolitic ignimbrites and lava flows of the Snake River Plain are typically crystal-poor with less than 20% phenocrysts of plagioclase, quartz, Fe–Ti oxides, Fe-rich pyroxenes, and in some sanidine (or anorthoclase). Biotite and hornblende are rare (e.g., Honjo et al. 1992; Cathey and Nash 2004; Wright et al. 2002; Kellogg et al. 1994; Manley and McIntosh 2002; Christiansen 2001). A few lava flows and tuffs also have fayalite (e.g., Spear 1979; Bonnichsen and Citron 1982; Christiansen 2001). Typical accessory minerals are apatite, zircon, chevkinite, and allanite. Snake River Plain basalts typically have olivine (with Cr-spinel inclusions) and plagioclase as the dominant phenocrysts. Augite is abundant in the groundmass along with plagioclase, magnetite, ilmenite, apatite, and olivine (Leeman and Vitaliano 1976; Stout and Nicholls 1977). Ferrobasalt to ferrolatite lavas in the Craters of the Moon volcanic field contain phenocrysts of clinopyroxene, apatite, and magnetite in the more silicic members of the suite (Leeman et al. 1976; Stout et al. 1994).

### Intensive parameters

The conditions of crystallization have been estimated for several of the silicic volcanic units in the Great Basin volcanic fields (Nielsen 1992; Maughan et al. 2001; Nusbaum 1990; Best et al. 1989; Ross et al. 2002; Radke et al. 1992; Phillips 1989). Dacites typically crystallized at

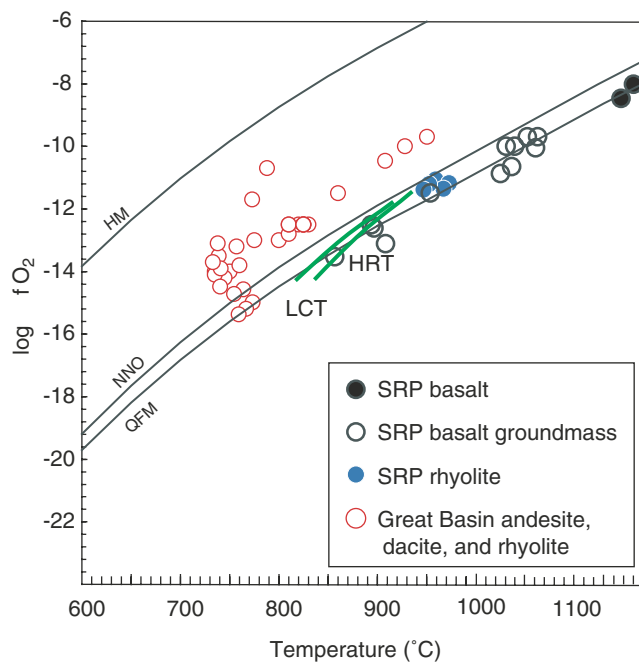


**Fig. 2** Temperature and oxygen fugacities for volcanic rocks from the Snake River Plain contrasted with those from the Indian Peak and Central Nevada volcanic fields. *LCT* Lava Creek Tuff and *HRT* Huckleberry Ridge Tuff, both from the Yellowstone caldera. *T* and *f*O<sub>2</sub> compiled from Hildreth (1981), Leeman and Vitaliano (1976), Stout and Nicholls (1977), Honjo (1990), and Christiansen (unpublished data)

2–3 log units above the QFM buffer at temperatures ranging from about 770 to 850°C (Fig. 2). Rhyolites crystallized at lower temperatures (about 725–780°C) and similar oxygen fugacities, with the exception of the Stone Cabin Formation and the fayalite-bearing member of the Shingle Pass Tuff which crystallized near the QFM buffer. Water fugacities were high enough to stabilize hydrous mafic silicates (i.e., 3–6 wt.% H<sub>2</sub>O), but the magmas were probably not water-saturated before eruption (Christiansen 2005b).

Mineral compositions in the Snake River Plains basalts (Leeman and Vitaliano 1976; Leeman et al. 1976; Stout and Nicholls 1977; Stout et al. 1994; Honjo and Leeman 1987, Putirka et al. 2003; and Christiansen's (2005) unpublished data for Kimama and Rocky Buttes) suggest that the lavas erupted at temperatures near 1,200°C and were crystallizing on or below the QFM oxygen buffer. The rhyolites of the Snake River plain likewise crystallized at low oxygen fugacities near QFM and at high temperatures for rhyolites of about 1,050°C to as low as 850°C (e.g., Honjo 1990; Hildreth 1981; Perkins et al. 1998; Cathey and Nash 2004). The lower temperature varieties may have Fe-rich biotite or hornblende (e.g., Christiansen 2001) indicating modest water contents (at least 2 or 3% H<sub>2</sub>O; Christiansen 2005b). Most of these cooler tuffs erupted from calderas in the eastern Snake River Plain and Yellowstone (Hughes and McCurry 2002).

## Major- and trace-element geochemistry

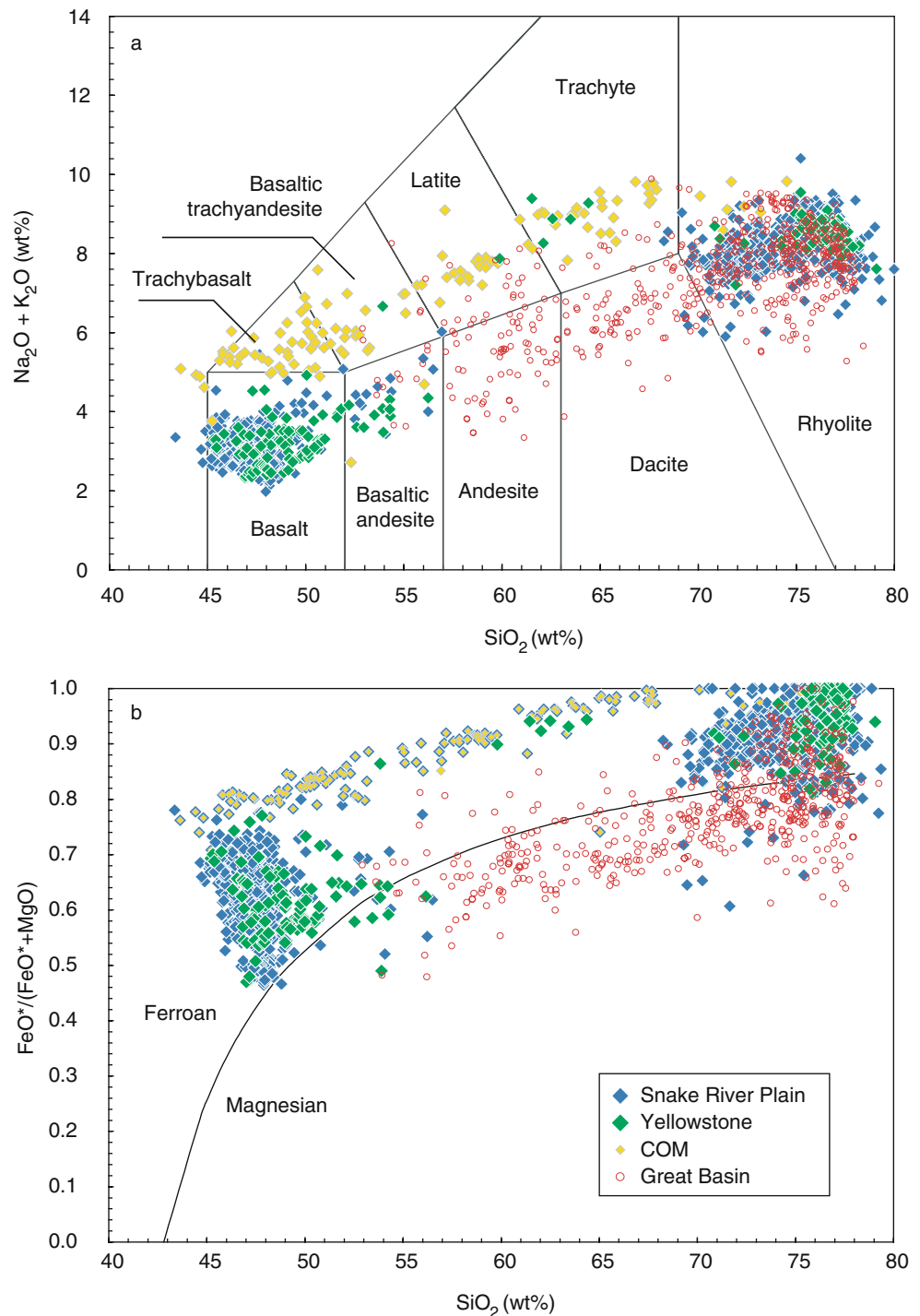
The major-element classifications of the volcanic rocks from the two contrasting regions are shown in Fig. 3. Rhyolites and basalts dominate the Snake River Plain. We have plotted Yellowstone rocks separately from the rest because they are distinctive in several respects (e.g., Hughes and McCurry 2002). Only a few basaltic andesites or andesites have been discovered thus far. Rare intermediate lavas follow a distinctly alkaline (alkali-calcic to alkaline using the MALI-modified alkali lime index-of Frost et al. 2001) chemical trend (see ESM Fig. 3c) and are grouped in our plots with their most voluminous representative, the lavas of the Craters of the Moon. This group also includes rhyolitic lava flows from Cedar Butte, East Butte, Big Southern Butte, Unnamed Butte, and a few samples from unknown vents acquired by drilling near the Idaho National Engineering and Environmental Laboratory in the central part of the Snake River Plain (McCurry et al. 1999, 2007). Silicic rocks from the Snake River Plain are overwhelmingly rhyolite, but span the range from low-to high-silica varieties. Basalts and rhyolites of the Snake River Plain rocks are tholeiitic (Fig. 3b) following Miyashiro's (1974) subdivision (or ferroan using the terminology of Frost et al. 2001). The rhyolites and basalts are mainly calcic to calc-alkaline, with the clear exception of those on the Craters of the Moon-Cedar Butte trend and a few rhyolites which are alkali-calcic to alkaline (see ESM Fig. 3c). The lavas of the Craters of the Moon-Cedar Butte trend are nonetheless silica saturated—like all the rocks considered here. Most of the rhyolites are high-K and the basalts medium-K (see ESM Fig. 3d) using the criteria of Ewart (1979).

The Oligocene suite from the Great Basin, on the other hand, includes no basalt (Fig. 3a). Basaltic lavas are no older than about 20 Ma in this part of the Great Basin (Christiansen 2005a). Instead, andesite is the most voluminous lava and dacite and rhyolite are the most voluminous pyroclastic rocks (Barr 1993; Best et al. 1993). Andesite and dacite are essentially absent from the Snake River Plain. Moreover, for a given silica content the Great Basin rocks have lower FeO/(FeO+MgO) ratios than those from the Snake River Plain (Fig. 3b). About half of the Oligocene rhyolites are ferroan, but the andesites and dacites are clearly magnesian (or calc-alkaline in the sense of Miyashiro 1974). Using the modified alkali-lime index (see ESM Fig. 3c), the Oligocene suite ranges widely from calcic to alkaline, but most of the dacites and rhyolites are calc-alkaline. With the exception of some of the most mafic lavas, this suite is dominantly high K<sub>2</sub>O (see ESM Fig. 3d), like the silicic suite on the Snake River Plain.

The two suites are different in several important aspects as summarized in the following discussion based on major element variations. Because we are mostly interested in the



**Fig. 3** Classification diagrams for the two volcanic suites discussed here. **a** Volcanic rocks from the Snake River Plain form a bimodal association. Rare intermediate to silicic rocks form the distinctive Craters of the Moon-Cedar Butte (COM) trend. The Great Basin suite is more diverse, ranging from basaltic andesite to high-silica rhyolite. All analyses with less than about 62% SiO<sub>2</sub> are lava flows. **b** Volcanic rocks of the Great Basin are mostly magnesian (i.e., calc-alkaline) but some of the most silicic are ferroan (i.e., tholeiitic), whereas the rocks of the Snake River Plain are consistently ferroan (dividing line from Miyashiro 1974). Rhyolites of the Snake River Plains (see ESM) are dominantly calc-alkaline on the modified alkali lime index of Frost et al. (2001) whereas the silicic rocks of the Great Basin range widely. Silicic rocks from both suites (see ESM) are high to very high K<sub>2</sub>O, but the basalts from the Snake River Plain are low to medium K<sub>2</sub>O



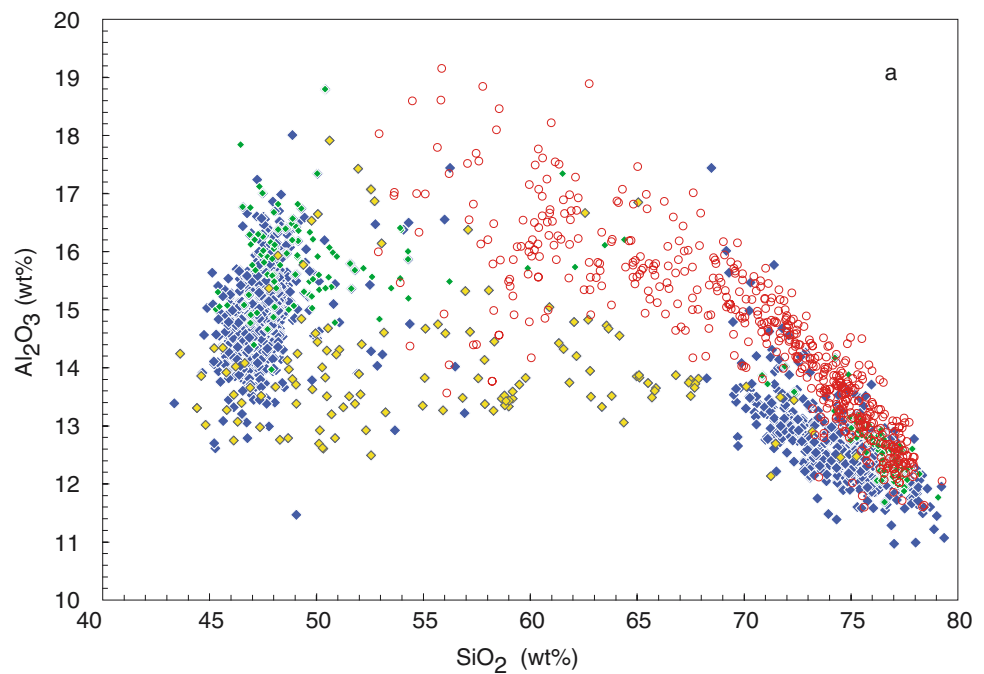
origin of the rhyolites, we generally illustrate these differences on silica variation diagrams.

#### Snake River Plain basalts

Typically described as Snake River Plain olivine tholeiites, the basalts follow classic tholeiitic differentiation trends on silica variation diagrams (Figs. 3, 4 and 5). There is a notable increase in FeO<sub>T</sub> (ESM Fig. 4c) and TiO<sub>2</sub> (Fig. 4b)

which accompanies a small but distinctive drop in silica (from 48 to 46% SiO<sub>2</sub>). Mn, K (ESM Fig. 3d), Rb, Ba (Fig. 6a), Pb, P, REE (ESM Fig. 6b), Y, Zr (ESM Fig. 6d), Nb, Ta, Th, Zn, and V (ESM Fig. 6f) all covary and are incompatible elements. Mg (ESM Fig. 5d), Ni, Cr, Al (ESM Fig. 4a), Ca (ESM Fig. 4d), and Sr (ESM Fig. 6a) decline with differentiation and are compatible elements in the basalts. Sc trends are variable with lavas from some volcanoes experiencing modest Sc increases with evolution

**Fig. 4** Major element variation diagrams comparing the volcanic rocks of the Snake River Plain with the Oligocene suite from the Great Basin. The Great Basin rocks have distinctly higher  $\text{Al}_2\text{O}_3$  (a), lower  $\text{TiO}_2$  (see ESM), lower FeO (see ESM), and higher CaO (see ESM) concentrations. The Snake River Plains basalts follow Fe and Ti-enrichment and Si-depletion trends quite different from the mafic rocks of the Great Basin suite



while others have declining Sc.  $\text{TiO}_2/\text{MgO}$  (ESM Fig. 5d), K/Na, and La/Yb all increase with evolution. In the Fe–Ti-rich basalts,  $\text{TiO}_2$  reaches as high as 4 wt.% (Fig. 4b). The enrichment in  $\text{TiO}_2$  in the most mafic rocks contrasts strongly with the Great Basin suite, the most mafic members of which have less than 2%  $\text{TiO}_2$ , typical of calc-alkaline magmas in general (Gill 1981).

The major and trace element variations in the basalts are consistent with the fractionation of the observed phenocrysts-olivine and plagioclase, joined in some magma

systems by clinopyroxene (Leeman et al. 1976; Leeman and Vitaliano 1976; Christiansen and Hurst 2004). In particular, declining MgO is consistent with olivine fractionation and declining Sr, CaO,  $\text{Al}_2\text{O}_3$ , and  $\text{SiO}_2$  show the importance of plagioclase fractionation at low pressure. Fractionation of small proportions of spinel is needed to explain the strong Cr depletion, but magnetite and ilmenite fractionation were limited as indicated by the increase in Ti, V, and Fe. The role of clinopyroxene fractionation seems to vary from volcano to volcano as indicated by Sc variations.

**Fig. 5** Mg–Fe relations reveal the differences and interrelationships of the two suites of rocks considered here. a The Ti-depletion trend distinguishes the magnesian rocks of the Great Basin from the ferroan Snake River Plains rocks. Rhyolites of the Great Basin (see ESM) have the highest MgO concentrations. The Craters of the Moon-Cedar Butte-rocks are very MgO depleted and unlike typical rhyolites of the Snake River Plain. For FeO and MgO (see ESM), a link between highly evolved basalts and the Craters of the Moon-Cedar Butte-trend is apparent. The Great Basin suite (see ESM) also has low  $\text{TiO}_2/\text{MgO}$  ratios

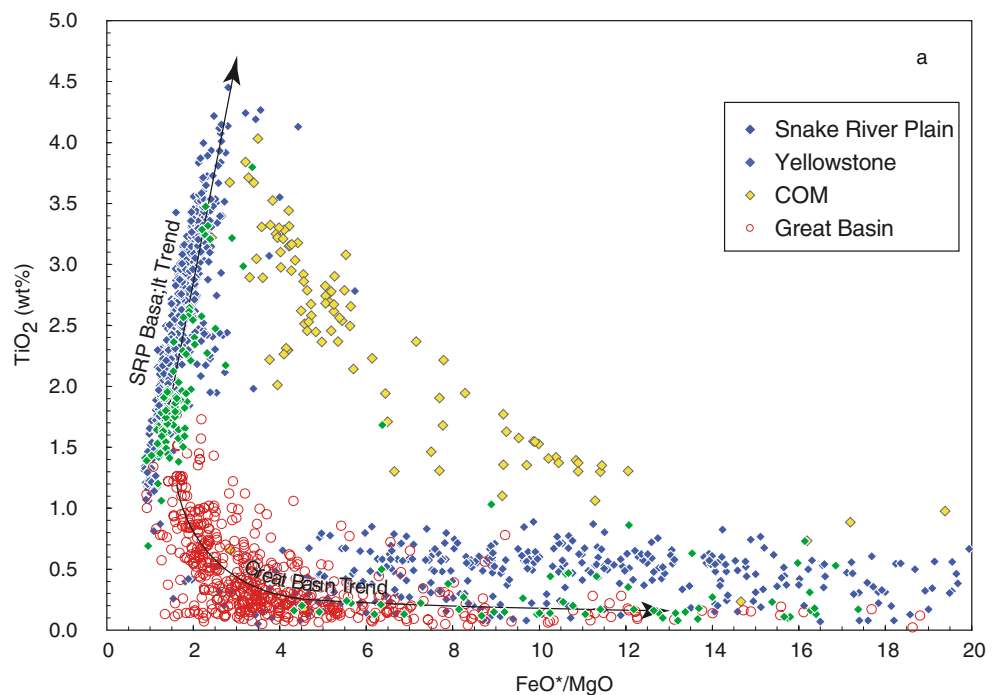
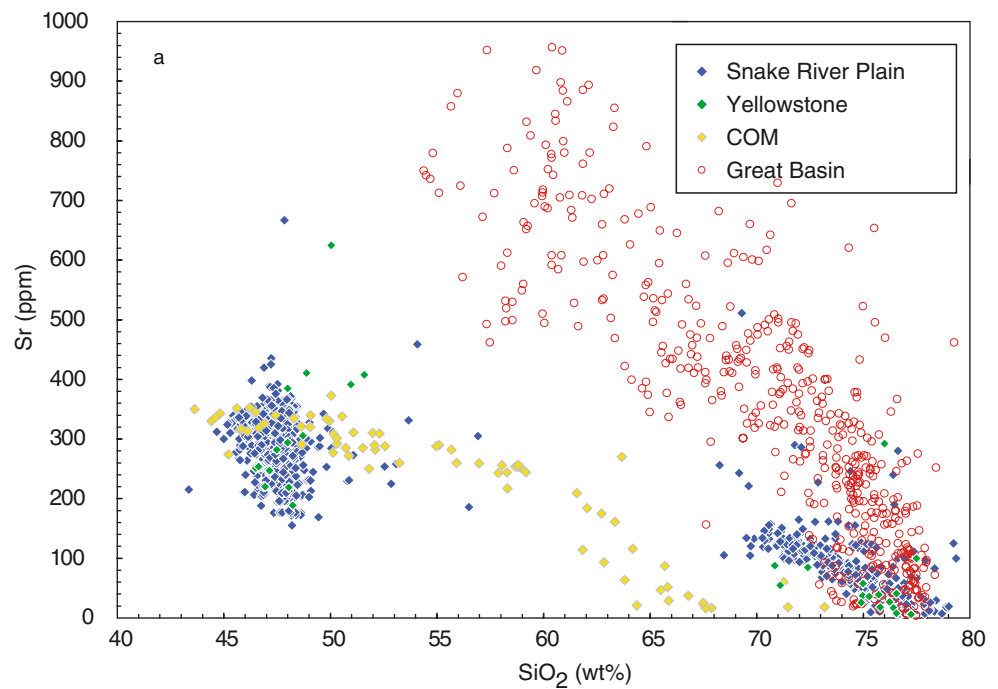


**Fig. 6** Trace element variation diagrams for volcanic rocks from the Snake River Plain and Great Basin. **a** SiO<sub>2</sub>–Sr. See ESM for SiO<sub>2</sub>–Ce, SiO<sub>2</sub>–Ba, SiO<sub>2</sub>–Zr, La/Nb (or La/Ta where Nb was not analyzed) ratios normalized to primitive mantle (McDonough and Sun 1995) versus SiO<sub>2</sub>, and V–TiO<sub>2</sub>



Few if any of the basalts on the Snake River Plain are primary, as indicated by high Fe/Fe+Mg ratios and low concentrations of Ni (<300 ppm) and Cr (<550 ppm).

#### Yellowstone basalts

The basalts of the Yellowstone region share many of their characteristics with the rest of the Snake River Plain, but basalts from Yellowstone with high TiO<sub>2</sub> are rare compared to basalts from elsewhere on the plain (Fig. 4b). Less than 10 of the 200 or so basaltic rocks from Yellowstone have TiO<sub>2</sub> that is higher than 2.5%. In contrast, about half of the samples from the rest of the Snake River Plain have higher concentrations of TiO<sub>2</sub> > 2.5%. Moreover, mafic lavas near Yellowstone include distinctive basalts and basaltic andesites with higher SiO<sub>2</sub> (Figs. 3 and 4) and low MgO (ESM Fig. 5d). A few of these fall into the magnesian field in Fig. 3b. Mixing of a relatively unevolved basalt (MgO ~ 9% and TiO<sub>2</sub> ~ 2%) with rhyolite can explain most trends on the variation diagrams (Figs. 3, 4 and 5). The close association of these basalts with an active rhyolite magma system is the most likely explanation for these differences. Most other basalts in our data set erupted millions of years after rhyolite magmatism became inactive.

#### Relation of basalts to rhyolites

Snake River Plain basalts become highly fractionated but erupted rocks do not trend toward rhyolite, except for the Craters of the Moon-Cedar Butte trend (e.g., Figs. 3b and 4b). Instead, a large silica gap between the voluminous

rhyolites and the basalts suggests these rhyolites are not derived by fractional crystallization of basalt.

#### Craters of the Moon-Cedar Butte trend

The Craters of the Moon-Cedar Butte trend is a distinctive alkaline suite of silica-saturated to oversaturated lavas. The lavas extend from trachybasalts through trachyandesites and include a few trachydacite and rhyolite lava flows (Fig. 3a). Individual flows have small volumes and no ignimbrites from this trend have yet been found. The lavas have been identified mostly along the margins of the plain and along the Great Rift of the Craters of the Moon (Leeman et al. 1976), but the rocks of Cedar Butte and nearby rhyolite domes (McCurry et al. 2007) follow the same differentiation path. A few intermediate composition lavas from the Yellowstone region, notably the trachyandesites of High Point (Christiansen 2001) also follow this trend, but are plotted with the other Yellowstone rocks for consistency.

The lowest silica lavas on the Craters of the Moon-Cedar Butte trend overlap with the evolved Fe–Ti basalts for some major elements, including Fe (see ESM Fig. 4c), Al (see ESM Fig. 4a), and Mn, but the most mafic members are far more enriched in P<sub>2</sub>O<sub>5</sub> (to as much as 3% in the most mafic samples) and K<sub>2</sub>O (see ESM Fig. 3d) and to a lesser extent Na<sub>2</sub>O than the most evolved basalt. Moreover, the variation diagrams in Fig. 4 show they are lower in Mg and Ca than evolved Snake River Plain basalts, but Fe, Ti, Al, and Mn overlap for the two trends.

The Craters of the Moon-Cedar Butte trend is very different from the other volcanic rocks of the Snake River

Plain. It is marked by strong silica enrichment and FeO, TiO<sub>2</sub>, MgO, CaO, and P<sub>2</sub>O<sub>5</sub> depletion (Figs. 4 and 5). Al<sub>2</sub>O<sub>3</sub> and MnO are scattered but rise and then fall with silica enrichment. Among the trace elements Ba, REE, Rb, Y, Nb, Th, and Pb are strongly enriched along with silica (Fig. 6). Eu, although enriched compared to Snake River Plain basalts, varies little across the Craters of the Moon trend. Ni, Cr, P, V (ESM Fig. 6f) and Sr (ESM Fig. 6b) are strongly depleted as silica increases, and Sc concentrations are scattered but also decline. Zr and Ba are both incompatible in the intermediate members of the series, but in rocks with more than about 60 to 63% SiO<sub>2</sub>, both decline (Fig. 6). As concluded by Leeman et al. (1976), these elemental variations are consistent with fractionation of plagioclase, apatite, olivine, clinopyroxene, magnetite (Cr-rich). Since clinopyroxene crystallizes at moderately high pressures (Thompson 1975) in Snake River Plain basalt, this trend may only form by mid-crustal differentiation (Leeman et al. 1976; Stout et al. 1994). Oxide fractionation probably promotes the silica enrichment trend. The decline of Zr and Ba (Fig. 6) are probably the result of zircon and potassic feldspar (anorthoclase or sanidine) saturation in the more felsic magmas. Potassic feldspar fractionation is also responsible for the Al-depletion above about 60% SiO<sub>2</sub> (see ESM Fig. 4a). The strong depletion of V compared to Ti suggests that ilmenite fractionation was important for the Craters of the Moon-Cedar Butte trend (ESM Fig. 6f). However, Leeman et al. (1976) only found ilmenite as a groundmass phase in the ferrobasalts. The presence of crustal xenoliths and xenocrysts and the Sr isotopic compositions of the lavas from Craters of the Moon show that crustal contamination accompanied fractional crystallization (Leeman et al. 1976). However, the Nd isotopic ratios of rhyolites that lie on the Craters of the Moon-Cedar Butte trend (from Cedar Butte, Unnamed Butte, East Butte and Big Southern Butte) are the highest of all the rhyolites (Fig. 7), suggesting that assimilation of upper crustal materials was not required for the generation of the silicic rocks on the Craters of the Moon-Cedar Butte trend (Stout et al. 1994; McCurry et al. 2007).

Of considerable importance here is the relationship between the voluminous Snake River Plain rhyolites and the lavas on the Craters of the Moon-Cedar Butte trend. The silicic end of the differentiation trend overlaps with the Snake River Plain rhyolites for MnO, Al<sub>2</sub>O<sub>3</sub>, FeO, and K<sub>2</sub>O, and with TiO<sub>2</sub> for the low TiO<sub>2</sub> rhyolites of Yellowstone (Figs. 4, 5 and 6). On the assumption that Rb is completely incompatible, the most mafic Craters of the Moon magma would have experienced about 80% crystallization to reach the composition of the low-silica rhyolites. However, the low MgO, CaO, P<sub>2</sub>O<sub>5</sub>, TiO<sub>2</sub>, Sr, and Ba and high Na<sub>2</sub>O and FeO/MgO, Pb and REE of the silicic rocks on COM-trend (Figs. 4, 5 and 6) show that this differentiation trend does not produce the voluminous rhyolites of the Snake River Plain. This is

particularly clear for FeO–MgO–TiO<sub>2</sub> relations (Figs. 3b and 5). We conclude that the typical voluminous rhyolites of the Snake River Plain and those on the Craters of the Moon-Cedar Butte trend have independent origins.

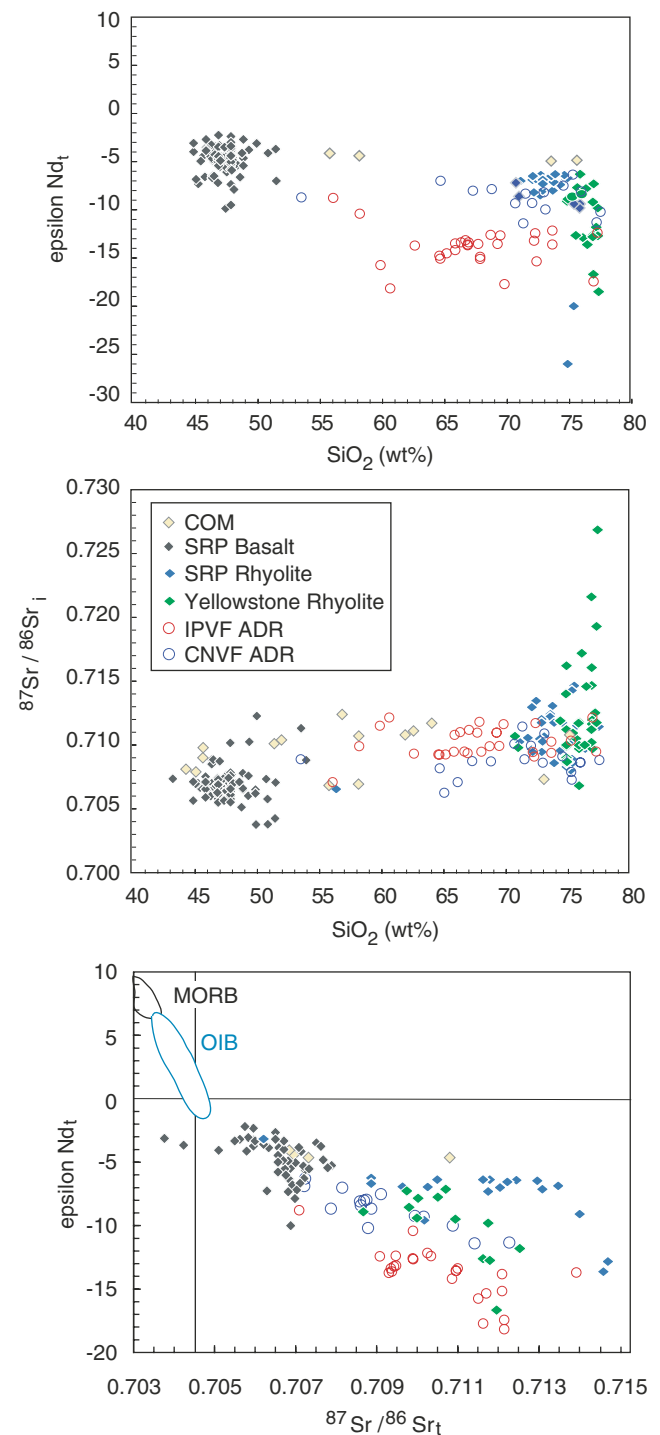


**Fig. 7** Initial Sr and Nd isotopic compositions of volcanic rocks from the Snake River Plain and from the Indian Peak and Central Nevada volcanic fields compared to midocean ridge basalt (MORB) and ocean island basalt (OIB). IPVF ADR are samples of andesite, dacite, and rhyolite from the Indian Peak volcanic field and CNVF ADR are samples of the same from central Nevada



Several of the major element trends (e.g. Fig 4b, ESM Fig. 4b, c, 5b–d) imply a continuation magmatic connection between the Snake River Plain basalts and the lavas of the Craters of the Moon-trend. Crystallization of Fe–Ti oxides (probably titanomagnetite) started at this juncture as indicated by kinks in the FeO and TiO<sub>2</sub> curves and onset of silica enrichment. However, there are significant gaps in the incompatible trace element trends (Fig. 6a, ESM Fig. 6b, d), that require about 50% crystallization of the most evolved Snake River Plain basalt to reach the composition of the least evolved trachyandesite on the Craters of the Moon trend. Reconciling the major and trace element data is difficult, but crystallization of plagioclase, olivine, clinopyroxene, and a Cr–Fe–Ti oxide in proportions that created cumulates with SiO<sub>2</sub> concentrations similar to the residual melts could cause enrichments and depletions of trace elements, but cause little change in silica. Because P, Zr, Y, and REE behave incompatibly, apatite, zircon, or other accessory minerals were apparently not stable during this part of the differentiation history. If the Craters of the Moon-Cedar Butte-trend is related to differentiation of Snake River Plain basalt, the “missing” intermediate magmas may have been too Fe-rich and dense to erupt. Once magnetite precipitation drove residual magmas to become SiO<sub>2</sub> enriched and less dense, eruptions of small volumes of highly differentiated magma are possible (Fig. 8).

#### Snake River Plain rhyolites

As noted before, rhyolites of the Snake River Plain range from low to high silica, are almost all ferroan, and medium

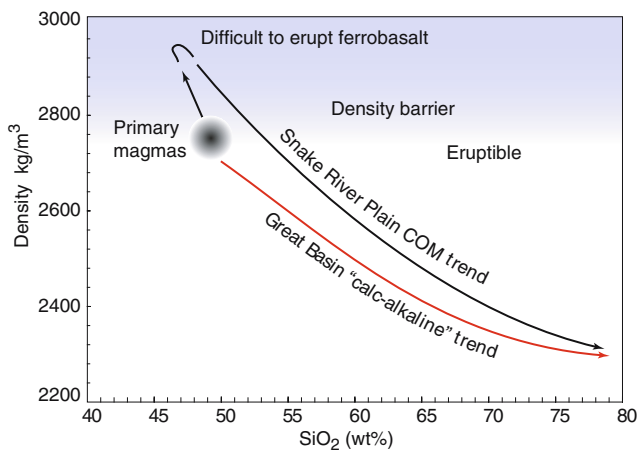


**Fig. 8** Schematic plot of magmatic density versus silica for magnesian series from the Great Basin as compared to the ferroan trend for Snake River Plain magmas. Differentiation of low  $f_{O_2}$  Snake River Plain basalt produces Fe-rich dense magma which may be too dense to erupt. Once magnetite precipitates, its fractionation lowers FeO and enriches SiO<sub>2</sub> in residual liquids as on the Craters of the Moon-Cedar Butte (COM) trend which may lead to small volumes of rhyolite. Differentiation of a high  $f_{O_2}$  magnesian magma series produces continuous silica increases and density decreases

to high K<sub>2</sub>O (Fig. 3). Thus, the rhyolites have all of the classical characteristics of A-type granites, including high concentrations of alkalis, especially as compared to aluminum, high Fe/Mg, and TiO<sub>2</sub>/MgO ratios, as well as high concentrations of incompatible elements and especially those with high field strength such as Nb, Ta, Zr, and Th. Their patterns on chondrite-normalized trace element diagrams lack the large negative Nb anomalies of subduction-zone rhyolites and they consequently have low La/Nb ratios (ESM Fig. 6e). They also plot solidly inside the within plate granite field on the discrimination diagrams of Pearce et al. (1984) as a result of high Nb and Y concentrations (Fig. 9). The rhyolites also have many of the mineralogical characteristics of A-type magmas, including high temperatures and anhydrous mineral assemblages. In these latter characteristics they are markedly different from the topaz rhyolites of the Basin and Range province with which they are contemporaneous (Christiansen et al. 1986).

Evolutionary patterns in the Snake River Plains rhyolites are marked by depletion of Sr (ESM Fig. 6a), Eu (ESM Fig. 11), Sc (ESM Fig. 11), V (ESM Fig. 6f), Cr (ESM Fig. 11), Ni (ESM Fig. 11), Zr (ESM Fig. 6d), Hf, Zn (ESM Fig. 11), Y (ESM Fig. 11), Ti (Fig. 4b), Al (ESM Fig. 4a), Fe (ESM Fig. 4c), Mn, Mg (Fig. 5a), Ca (ESM Fig. 4d), P (ESM Fig. 11) and enrichment of K (ESM Fig. 3d), Rb (ESM Fig. 11), Th (ESM Fig. 11), U (ESM Fig. 11), and HREE (ESM Fig. 11). These trends can be explained by fractionation of the observed phenocryst phases—plagioclase, quartz, pyroxenes, Fe–Ti oxides, zircon, apatite. Potassium (ESM Fig. 3d), Ba (Fig. 6c, ESM Fig. 11), and LREE (ESM Fig. 6b) are depleted

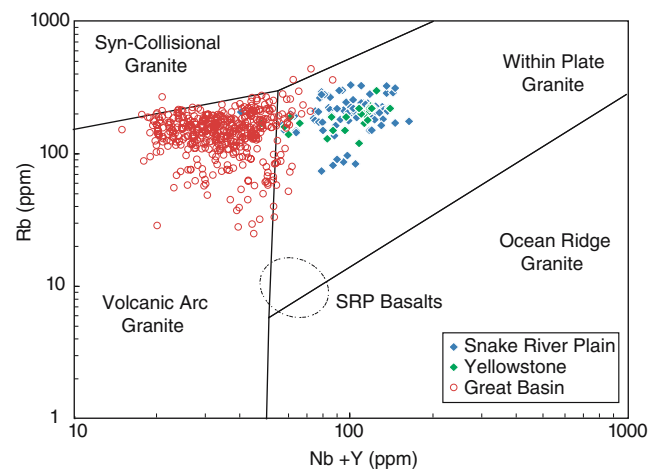


**Fig. 9** The Snake River Plain rhyolites plot consistently in the Within Plate Granite field on the discriminant diagram of Pearce et al. (1984). With a few exceptions described in the text, the silicic rocks of the Oligocene suite from the Great Basin fall within the Volcanic Arc field, consistent with their clear link to subduction of the Farallon plate during the Oligocene. The compositions of the basalts from the Snake River Plain are shown for reference only

in the most evolved, lowest temperature rhyolites probably as a result of sanidine (and biotite in a few systems) and chevkinite or allanite fractionation.

Beyond the large scale similarities there are some differences in the composition of the rhyolites as a function of age and location. For example, Perkins and Nash (2002) concluded that the FeO content (and degree of evolution) of the rhyolitic magma systems waxed and waned with time. FeO content and temperature peaked 10 Ma in rhyolites erupted from near Twin Falls (Nash et al. 2006). Hughes and McCurry (2002) contend that the rhyolites east of about 114° longitude are slightly different than their western counterparts. For example, low-silica rhyolites are rare in Yellowstone compared to the rest of the Plain (Figs. 3 and 4). Rhyolites with less than 74% SiO<sub>2</sub> (Fig. 5a) and more than 2.5% FeO are rare among the rocks analyzed from Yellowstone (ESM Fig. 5c). As a consequence, an average Yellowstone rhyolite has lower FeO<sub>T</sub>, MgO, CaO, K<sub>2</sub>O, P<sub>2</sub>O<sub>5</sub> and higher Al<sub>2</sub>O<sub>3</sub> and Na<sub>2</sub>O than average Snake River Plain rhyolite (exclusive of Yellowstone). The slight differences extend to trace elements (Fig. 6) as well, with the Yellowstone rhyolites lying on the high concentration end of differentiation trends for incompatible elements (e.g., Rb, Y, Nb, Th, U, REE) and on the low concentration end for compatible elements (e.g., Zr, Zn, Sc, V, Cr, Ni, Sr, Ba, Eu). There are few differences that cannot simply be attributed to lower temperatures or more extensive differentiation of the Yellowstone rhyolites. However, at a given Rb concentration, Sr, Zr, and Sc concentrations are lower in Yellowstone rhyolites. For example, a typical Yellowstone rhyolite with 175 ppm Rb has 50 ppm Sr versus 100 ppm Sr in a typical Snake River Plain rhyolite (see ESM Fig. 13b).

#### Oligocene silicic volcanic rocks from Great Basin

The Oligocene dacites and rhyolites of the Great Basin appear to be the silicic end of a long and continuous differentiation series that includes basaltic andesites and andesites, largely belonging to the magnesian (or calc-alkaline) series (Fig. 3b). The characteristics of these silicic rocks are clearest when contrasted with the rhyolites from the Snake River Plain. Many of the elements overlap at the highest silica concentrations. Thus, we compare the two suites at 70% SiO<sub>2</sub> and use the symbol E<sup>70</sup>, where E is the element or oxide of interest. It is worth noting that the differences between the two suites are not a result of greater phenocryst proportions in the Great Basin rocks; crystal-rich and crystal-poor rhyolites have indistinguishable compositions at this scale and both are included in the figures.

On silica variation diagrams the Great Basin dacites and rhyolites have significantly lower concentrations of FeO and TiO<sub>2</sub> than Snake River Plains rhyolites. For example, typical

Great Basin rocks FeO<sub>T</sub><sup>70</sup> is 3% and TiO<sub>2</sub><sup>70</sup> is 0.4%, whereas FeO<sub>T</sub><sup>70</sup> is 5% and TiO<sub>2</sub><sup>70</sup> is 0.8% in Snake River Plain rhyolites. As a consequence of the low TiO<sub>2</sub>, these Oligocene rhyolites also have much lower TiO<sub>2</sub>/MgO ratios—a parameter used by Patiño Douce (1997) to distinguish between “calc-alkaline” and anorogenic silicic magmas. In addition, Zn, REE, Y, Zr, Ta, Nb are significantly lower in these magnesian rocks, as is the La/Nb ratio (ESM Fig. 6e). (In the most evolved Great Basin rhyolites in which allanite or chevkinite fractionation was important, La/Nb ratios are lower and overlap with the Snake River Plain rhyolites, e.g., Radke et al. 1992, Nielsen 1992.) As a result, most of the silicic rocks from the Great Basin plot in the “volcanic arc” field (Fig. 9) on the discriminant diagram of Pearce et al. (1984). A few hot Zr-rich rhyolites plot in the “within plate granite” field and include six samples of the Lamerdorf Tuff (Best et al. 1989). Typically, however, Zr<sup>70</sup> is about three times lower in the Oligocene series than in Snake River Plain rhyolites, consistent with the much lower eruption temperatures and lower solubility of zircon in the older suite (see ESM Fig. 6d).

The Oligocene dacites and rhyolites have much higher Sr (Sr<sup>70</sup> is 450 ppm in the older magmas versus 150 ppm in the younger ones), and significantly higher Al<sub>2</sub>O<sub>3</sub> (ESM Fig. 4a) and CaO (ESM Fig. 4a) than the Snake River Plain rhyolites. This suggests that plagioclase solubility was significantly higher in the hydrous, magnesian dacites and rhyolites of the Great Basin. In addition, Sr and Pb may have been added from a subduction-zirone fluid. The trace element patterns of dacites and rhyolites from the Great Basin reveal some of these features as well (ESM Fig. 11) with large negative Nb anomalies and higher Sr and Pb in the Oligocene suite compared to Snake River Plain rhyolites of comparable silica contents. Sc may be slightly higher in the magnesian suite than in the ferroan rocks of the Snake River Plain, perhaps as a result of enhanced fractionation of pyroxene in the dry Snake River Plain rhyolites, instead of biotite and hornblende in the Great Basin silicic magmas.

It is also revealing to consider those element trends which are not different between the two suites of silicic magmas. MnO, MgO, Na<sub>2</sub>O, K<sub>2</sub>O, P<sub>2</sub>O<sub>5</sub>, Rb, Th, Ni, Cr, Sc, Th, and U all have similar concentrations and trends on silica variation diagrams for the two suites of silicic rocks. Moreover, both suites plot in similar positions on the TAS diagram (Fig. 3) and have similar (Na<sub>2</sub>O+K<sub>2</sub>O)/Al<sub>2</sub>O<sub>3</sub>, K/Na, Ca/Al, and FeO/TiO<sub>2</sub> ratios.

#### Isotope geochemistry

The Snake River Plain region is probably underlain by Archean to Proterozoic age crust with very high <sup>87</sup>Sr/<sup>86</sup>Sr

(greater than 0.735) and low  $\epsilon\text{Nd}$  (less than  $-20$ ). Leeman et al. (1985) and Wolf et al. (2005) report Archean ages for xenoliths erupted as far west as Square Mountain in the central Snake River Plain. The western margin of the Precambrian craton probably is near the Idaho–Oregon border (Manduca et al. 1993; Nash et al. 2006). Accreted ocean floor terrains of Paleozoic and Mesozoic age lie to the west. The influence of the craton on the composition of volcanic rocks is shown by marked lowering of Nd isotope ratios in Snake River Plain fallout ash beds about 15 Ma as the suture moved over the Yellowstone hot spot (Nash et al. 2006).  $\epsilon\text{Nd}$  in silicic ash dropped from +4 in western rhyolite ashes to as low as  $-11$  in eastern rhyolites. The ancient basement provides strong isotopic leverage to monitor the role of continental crustal contamination in the generation of the Snake River Plain rhyolites. Many of the analyzed Snake River Plain rhyolites have Nd isotopic compositions ( $\epsilon\text{Nd}$  ranges from  $-5$  to  $-10$ ) that lie within the observed range for the basalts ( $\epsilon\text{Nd}$   $-4$  to  $-7.4$  with two outliers at  $-10$ ), but they are concentrated on the low end of the basalt range (Fig. 7). The low temperature, high- $\text{SiO}_2$  ( $>76\%$ ) rhyolites from near Yellowstone extend to much lower  $\epsilon\text{Nd}$  ( $-5$  to  $-20$ ). Basalts have initial  $^{87}\text{Sr}/^{86}\text{Sr}$  isotope ratios that cluster about 0.707 with several outliers (Fig. 7). Only a few of the rhyolites have Sr-isotope ratios this low; most are between 0.709 and 0.715, with the post-collapse rhyolites from Yellowstone extending to even higher ratios. In general, those rhyolites with the lowest Sr content also have the highest  $^{87}\text{Sr}/^{86}\text{Sr}$  ratios suggesting that crustal contamination occurs during differentiation of the rhyolites. The rhyolites on the Craters of the Moon–Cedar Butte trend have higher  $\epsilon\text{Nd}$  than any of the Snake River Plain rhyolites and initial Sr isotope ratios are rather low (McCurry et al. 1999, 2007). This is consistent with fractional crystallization being more important than crustal assimilation in the evolution of this distinctive magmatic trend.

The eastern portion of the Great Basin is underlain by poorly exposed Proterozoic lithosphere. The few basement samples that have been analyzed have  $\epsilon\text{Nd}$  values about  $-7$  to  $-22$  (average  $-17$ ) and highly variable Sr isotope ratios that average about 0.720 (Nelson et al. 2002). Therefore, the contrast between the Proterozoic basement and the mantle is smaller than for the Snake River Plain region where Archean crust is present. Figure 7 shows that dacites and rhyolites from the Indian Peak and Central Nevada volcanic fields have  $^{87}\text{Sr}/^{86}\text{Sr}$  (0.709 to 0.712) that largely overlap the silicic rocks of the Snake River Plain, but  $\epsilon\text{Nd}$  values ( $-14$  to  $-18$ ) are distinctly lower than for the rhyolites of the Snake River Plain (Hart 1997). The isotopic compositions of several post-collapse Yellowstone rhyolites overlap with the volcanic rocks from the Central Nevada volcanic field (Fig. 7). However, because of their distinctive  $\epsilon\text{Nd}$  values, only a few of the Snake River

Plain or Yellowstone rhyolites overlap with the volcanic rocks from the Indian Peak volcanic field. These relationships strongly indicate that a significantly smaller proportion of Precambrian crust is involved in the Snake River Plain rhyolites than in the Oligocene rocks of the Great Basin.

## Discussion

In this section, we outline contrasting models for the generation of silicic rocks in the Snake River Plain and the Oligocene rocks of the Great Basin. We trace most of the distinctive characteristics of the two suites to their contrasting mantle roots and their distinctively different volatile fugacities.

### Production of rhyolite by fractional crystallization

Like many other subduction-related magmatic arcs, the isotopic compositions (Nd, Sr, and O) and of the dacites and rhyolites of the Great Basin show that they cannot have evolved simply by fractional crystallization of mantle-derived basalt. The Nd crustal index (DePaolo et al. 1992) for the dacites and rhyolites of the Indian Peak volcanic field ranges from 1 to 0.8, assuming a crustal  $\epsilon\text{Nd}$  value of  $-17$ , the average composition of closest Precambrian basement exposures in the Wasatch Range of central Utah (Nelson et al. 2002).

However, several studies (e.g., Bonin 2005 and Whitaker et al. 2007) have concluded that some continental anorogenic rhyolites form by extended fractional crystallization of such basalt. Whitaker et al. (2007) have shown with a series of incremental experiments that progressive crystallization of tholeiitic basalt can produce residual melt similar to rhyolites of the Craters of the Moon trend. The experiments were conducted at 4.3 kb with an initial water content of 0.4 wt.%. McCurry et al. (2007) concluded that this model is also consistent with trace element data for the Cedar Buttes rhyolites since they lie on continuous compositional trends with the ferrobasalts and ferrolatites of the Craters of the Moon suite. These rhyolites also have high  $\epsilon\text{Nd}$  values (Fig. 7) indicating a more direct link to the basalts than for the other rhyolites.

If the Craters of the Moon trend is related to continued evolution of Snake River Plain basalt, the “missing” intermediate products may have been too Fe-rich and dense to erupt. Once magnetite precipitation drove the magmas to become  $\text{SiO}_2$  enriched and less dense, eruptions of small volumes of highly differentiated magma were again possible (Fig. 8). These rhyolites are small in volume and compositionally distinct from the main volumes of

rhyolite: this is not the main mechanism by which rhyolite is produced in the Snake River Plain.

#### Production of rhyolite by partial melting of continental crust

A-type granites and rhyolites are commonly interpreted to be the result of partial melting of continental crust (e.g., Frindt et al. 2004, Rämö and Haapala 1995; Patiño Douce 1997; Collins et al. 1982; Leeman 1982; Anderson and Morrison 2005; Hughes and McCurry 2002; Christiansen et al. 1986; King et al. 2001). However, where the isotopic contrast between old crust and mantle is large, it has been argued that a significant percentage (as high as 100%) of the silicic magmas must have come from the mantle (e.g., Bonin 2005; Ewart et al. 2004). Intermediate models call for the partial melting of mafic crustal rocks recently derived from the mantle to give mantle-like isotopic signatures by partial melting these new additions to the crust. For example, Hildreth et al. (1991) argue that the rhyolites of Yellowstone were derived by partial melting of variably differentiated mafic intrusions only recently lodged in the crust. They estimate that 25–65% by mass of the material in the rhyolite came from such sources. However, their models involving hybridization of average Yellowstone basalt with Archean tonalites to granites called for less than 20% crustal material. The high Sr and low Nd isotope ratios found in some of the post-caldera rhyolites of Yellowstone are most likely the result of late assimilation of upper crustal roof rocks (Hildreth et al. 1991; Bindeman and Valley 2001). Likewise, Cathey and Nash (2004) calculated a Nd crustal index (DePaolo et al. 1992) of 0.38 for the Cougar Point tuffs (average  $\epsilon\text{Nd} -7.6$ ) of the central Snake River Plain. They assumed that the crust had an  $\epsilon\text{Nd}$  of  $-15$  and mantle  $\epsilon\text{Nd}$  was  $-3$ . If the crustal  $\epsilon\text{Nd}$  is lower, as indicated by the eruption of some rhyolite with  $\epsilon\text{Nd} < -15$  and the compositions of some crustal xenoliths, then the crustal index would be even lower.

The results of this summary are consistent with this latter interpretation involving a magma source dominated by juvenile mantle-derived material. The overlap in the isotopic composition of basaltic rocks and rhyolites of the Snake River Plain argues strongly for some type of “co-genetic” origin. But the large silica gap between the basalts and the rhyolites and the chemical inconsistencies noted above argue that there is not a continuous liquid line of descent for the large volume rhyolites from the basalts. Instead, we concur with Frost and Frost (1997) that the rhyolites of the Snake River Plain are derived by partial melting of their dry, tholeiitic, relatively reduced basaltic forerunners. Once basalt stalled in the crust because of density or strength contrasts and crystallized to form a

variable differentiated and contaminated gabbroic complex, subsequent intrusions could heat and partially melt the gabbro-crust hybrid to make hot silicic magma which could rise, accumulate and differentiate further in the shallow crust. Spulber and Rutherford (1983) produced rhyolitic melts with the major element characteristics of Snake River Plain rhyolites (including high  $\text{TiO}_2/\text{MgO}$  ratios, high FeO and  $\text{Na}_2\text{O}$ ) by small degrees of melting of tholeiitic basalt.

What was the composition of the partial melt parental to the Snake River Plain rhyolites? Hildreth et al. (1991) argued that a “...voluminous ‘dacitic’ (*sensu lato*) hybrid magma is stored beneath...” Yellowstone rhyolite magma. The evidence presented here suggests that the most mafic silicic magma generated by partial melting was a low-silica rhyolite. Streck and Grunder (2007) come to a similar conclusion for the hot, Fe-rich rhyolites of the High Lava Plains of Oregon. We identify this parental rhyolite magma on the basis of high Ba concentrations which produce flat normalized patterns for the most incompatible elements, Rb–Ba–Th–U (ESM Fig. 11). Such parental rhyolites erupted throughout the history and across the entire Snake River Plain and, though not common in Yellowstone, form part of the Huckleberry Ridge Tuff (Christiansen 2001). More differentiated rhyolites have lower Ba and negative Ba spikes on normalized trace element diagrams (see ESM Fig. 11). Ba is depleted by the fractionation of potassic feldspar, and in the lowest temperature rhyolites extreme Ba depletion is probably the result of combined sanidine and biotite fractionation (Fig. 6a).

In contrast, the dacites and rhyolites of the Great Basin are not part of a bimodal series and do not appear to be direct partial melts of the crust. They appear to have a direct liquid lineage with mantle-derived mafic magmas, albeit it a torturous open-system differentiation path involving hybridization with Proterozoic crust and extensive magma mixing along with crystal fractionation. Significant crustal contamination of mafic magma is consistent with the wide range of O- and Sr-isotopic compositions (Hart 1997). The parental magmas were probably less dense, wetter, cooler, and more oxidized than the Snake River Plain magmas and thus followed different crystallization paths.

*Trace element tests of partial melting models* Simple trace element models of partial melting in the crust are described in the Electronic Supplementary Material. The trace element models show that it is unlikely that the Snake River Plains rhyolites were derived by partial melting of upper crustal rocks or of lower crustal granulite. Instead, small degree melts of gabbroic equivalents of the basalt more closely match the Rb, Th, U, and Pb as well as the Ba/Rb and Pb/Ce ratios of the Snake River Plains rhyolites.



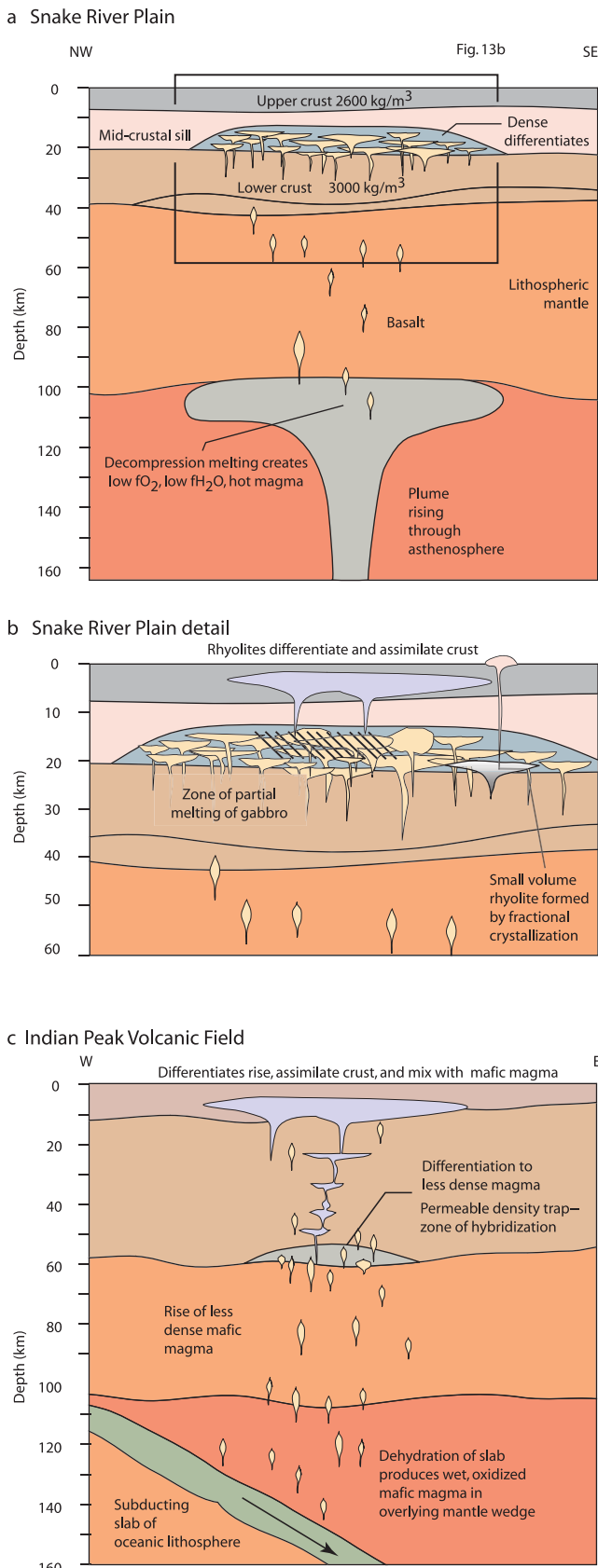


**Fig. 10** Schematic lithospheric cross-sections for the Snake River Plain (a and b) and for the Great Basin (c) about 30 Ma emphasizing the contrasts between the plume and subduction origins of the two magma suites

Magma density, state of stress, and contrasting evolution of lithospheric magma systems

Based on the constraints and calculations described above, we outline two different scenarios for magma generation that might explain the differences between the Snake River Plain rhyolites and the Oligocene Great Basin suite (Fig. 10). We suggest that Snake River Plain olivine tholeiite magmas stagnate in the middle crust where their magma pressure and buoyancy are insufficient to overcome the strength of crust. The density calculated for unevolved basaltic magma with 10% MgO is about 2,800 kg/m<sup>3</sup>. Sparlin et al. (1982) and Smith and Braile (1994) estimate that the lower crust has a density of about 3,000 kg/m<sup>3</sup> and the middle crust has a density of 2,670 kg/m<sup>3</sup> beneath the flanks of Snake River Plain. If this density structure represents the pre-magmatic character of the crust beneath the Snake River Plain, then basalt magma might stagnate at the boundary between the lower and middle crust. There, basalt magma could differentiate to a denser Fe-rich magma (2,800–2,900 kg/m<sup>3</sup>) that remains trapped because the residual magma is not buoyant. The magmas probably crystallize to form a plexus of sills and dikes filled with variably evolved gabbro, ferrogabbro, and ferrodiorite—the “mid-crustal sill.” Only a very small amount of differentiated rhyolitic magma has sufficiently low density (~2,400–2,200 kg/m<sup>3</sup>) to escape the density trap, rise, and erupt. The rhyolites at Cedar Butte may have formed by fractional crystallization in this type of magma system.

Parental magmas of the typical Snake River Plain rhyolites appear to form when enough hot mafic magma is inserted into the mid-crustal sill complex so that gabbroic rocks partially melt to form low density rhyolite magma (~2,400 kg/m<sup>3</sup>). This silicic magma has enough buoyancy to overcome the strength of the crust and rise out of the mid-crustal sill and through the middle and upper crust (<2,700 kg/m<sup>3</sup>). Cooling in the upper crust may retard the rise of magma and create shallow-level chambers from which rhyolite erupts to form large Yellowstone-type calderas. In these shallow chambers, magma could further differentiate to make low temperature, more highly evolved rhyolite magma. It is conceivable that relatively small aliquots of hot unevolved rhyolite may erupt directly from the gabbro melting zone, as hypothesized by Ekren et al. (1984) and Hughes and McCurry (2002). These may form lava flows or ignimbrites that lack clearly defined calderas.

A rather different story can be constructed for the parental magmas for the Great Basin suite (Fig. 10). Here, the parental magmas appear to have formed above a subducting slab of dehydrating oceanic lithosphere. These magmas probably had slightly lower densities than Snake River Plain tholeiite magmas because of their higher Al<sub>2</sub>O<sub>3</sub> and H<sub>2</sub>O and lower FeO contents. For example, the most

Mg-rich basaltic andesite from the Indian Peak volcanic field has a calculated magma density of  $\sim 2,600 \text{ kg/m}^3$ , assuming that it had 1%  $\text{H}_2\text{O}$  and was at its liquidus temperature. A hypothetical parental basalt, estimated by extrapolating elemental trends back to 50% silica, would have a slightly higher magmatic density of  $\sim 2,680 \text{ kg/m}^3$  assuming 1%  $\text{H}_2\text{O}$ ; even assuming no  $\text{H}_2\text{O}$ , its calculated magmatic density ( $\sim 2,730 \text{ kg/m}^3$ ) is still less than for the tholeiitic magmas of the Snake River Plain. As a result of their slightly lower densities, these “calc-alkaline” magmas may have stagnated higher in the crust where their buoyancy matched the strength of the crust. Even more important than their initial density is the fact that these higher  $f\text{O}_2$  magmas differentiated to Fe-poor melts that are less dense than their parents. Differentiation generated buoyant residual liquids which rose even higher into the crust. In this case, a mid-crustal density barrier would be semipermeable because evolved magmas could escape. As a result of this gradual density evolution, differentiating magma may have risen continuously, encountering and assimilating “fertile” crust on its rise path and becoming very contaminated as a result.

The state of stress in the lithosphere can exert a similar effect on basaltic magma systems (Best and Christiansen 2001; Marrett and Emerman 1992). In a compressional regime, such as the one that probably characterized the western US during the Oligocene ignimbrite flareup (Best and Christiansen 1991), the minimum horizontal stress direction ( $\sigma_2$ ) in the lower part of the brittle upper crust is less than the pressure exerted by magma rising from the mantle. Consequently, magma ascent is prevented and sills form within the brittle crust. If differentiation leads to less dense magma, the evolved magma could escape from the sill complex and continue to rise as depicted in Fig. 10.

#### Importance of intensive parameters

Many of the compositional and physical properties of these contrasting magma systems are probably the result of contrasts in their intensive properties, which were in turn established by distinctive tectonic settings. For example, temperature controls the distinctively high concentrations of Zr and Hf in the Snake River Plain rhyolites (Fig. 6) because the solubility of zircon is positively correlated with temperature (Watson and Harrison 1983). Higher temperature and lower  $f\text{O}_2$  in Snake River Plain rhyolites (Fig. 2) may also increase the solubility of magnetite and ilmenite compared to the cooler and more oxidized Great Basin dacites and rhyolites, thus increasing the FeO and  $\text{TiO}_2$  concentrations in rhyolite melts of otherwise similar composition.

High temperatures of the silicic Snake River Plain magmas are probably the result of relatively dry melting

of their source rocks. For example, mafic rocks with amphibole or biotite begin melting between about 750 and 875°C (e.g., Wolf and Wyllie 1995; Rapp and Watson 1995), whereas dry gabbro melts at temperatures of about 1100°C in the middle crust. Water in the source regions of the subduction-related Oligocene magmas produced melts at lower temperatures, a feature that was subsequently passed on to derivative magmas. The relatively high water fugacities kept the low temperature magmas molten to lower temperatures (Christiansen 2005b).

Patiño Douce (1997) attempted to use major element variation diagrams to distinguish between “calc-alkaline” and anorogenic granitic rocks. Of the discriminants he used, only the  $\text{TiO}_2/\text{MgO}$  effectively discriminates between the A-type rhyolites of the Snake River Plain ( $\text{TiO}_2/\text{MgO} > 1$ ) and the “calc-alkaline” rhyolites of the Great Basin ( $\text{TiO}_2/\text{MgO} < 1$ ; see ESM Fig. 5d). Patiño Douce (1997) experimentally produced rhyolitic melts with high  $\text{TiO}_2/\text{MgO}$  ratios by partially melting a “calc-alkaline” granodiorite at 4 kb and 950°C. We suggest that the high  $\text{TiO}_2/\text{MgO}$  ratios in the experimental liquids were not the result of low pressure melting, but of the low the oxygen fugacity in the experiments (estimated to be 1 log unit below QFM because of graphite in the cell assemblies). Low  $f\text{O}_2$  retards the crystallization of titaniferous magnetite and causes the  $\text{TiO}_2/\text{MgO}$  ratio to be rather high in the partial melt. Thus, these experiments show low  $f\text{O}_2$  raises the  $\text{TiO}_2/\text{MgO}$  ratio in partial melts and otherwise do not place significant constraints on the composition of the source materials or pressures of melting that produce A-type rhyolites. Such low  $f\text{O}_2$ s are unlike those found in natural calc-alkaline magma systems which are typically oxidized. Partial melting of an oxidized source should imprint the derived magma with a high  $f\text{O}_2$  as well (Carmichael 1991).

Water has also played an important role in the origin and evolution of the two rhyolite types. In contrast to the Snake River Plain Rhyolites, hydrous minerals in the Great Basin magma series are common and were stabilized by higher water fugacities and lower temperatures. In addition,  $\text{Al}_2\text{O}_3^{70}$  is about 13.5% in typical Snake River Plain rhyolite and about 14.5% in the Great Basin suite. Significantly higher concentrations of CaO are also present in the Great Basin series (Fig. 4d). These observations suggest plagioclase was more soluble in the Great Basin magmas as a result of higher water content.

In addition, distinctively high concentrations of Sr and Pb in the hydrous magmas of the Great Basin may be the result of their solubility in subduction zone fluids (e.g., Keppler 1996). As noted earlier, partial melting in a fluid-soaked wedge probably produced the mafic magmas that were parental to the Great Basin suite. Moreover, the enhanced solubility of plagioclase in wet magma retarded the depletion of Sr in the evolving magma.

## Conclusions

Silicic magmas from the Snake River Plain and the Great Basin contain distinctive fingerprints imposed by their different mantle parents. The Great Basin dacites and rhyolites were generally oxidized ( $fO_2 > NNO$ ), wet (high  $fH_2O$ ), cool, Sr- and Al-rich, and Fe-poor and part of an extended compositional trend from rhyolite to basaltic andesite. This is interpreted to reflect the derivation of their mafic parents from dehydration of subducting oceanic lithosphere that induced melting in the overlying wedge of mantle. Plagioclase fractionation was minimized by the high water fugacity and oxide precipitation was enhanced by high oxygen fugacity. This resulted in the formation of Si-, Al-, and Sr-rich differentiates that also have low Fe/Mg ratios and relatively low temperatures. Magma mixing, large proportions of crustal assimilation, and polybaric crystal fractionation were all important processes in generating the variety of silicic magmas erupted during this Oligocene ignimbrite flareup.

On the other hand, most of the rhyolite magmas of the Snake River Plain crystallized at low  $fO_2$  (near QFM), and are relatively hot, dry, Al- and Sr-poor, and Nb- and Fe-rich. The voluminous rhyolite is not part of a continuous differentiation trend, but bimodal with basalt. These characteristics were largely imposed by the derivation of parental basalts from a plume (or from the overlying lid of lithospheric mantle) having low  $fH_2O$  and low  $fO_2$ . These intensive parameters caused early precipitation of plagioclase (a consequence of low  $fH_2O$ ) and retarded crystallization of Fe–Ti oxides (because of the low  $fO_2$ ). These characteristics were passed on to their silicic partial melts which resulted from renewed intrusions of basalt magma. Partial melting of relatively dry gabbro also requires high temperatures. Subsequent fractionation of the rhyolitic magma led to the array of compositions found on the Snake River Plain province. Minor assimilation of continental crust also occurred during rhyolite genesis and differentiation, as indicated by moderately lower  $\epsilon Nd$  and higher initial Sr isotope ratios in the most evolved rhyolites.

We note in closing that our model for the origin of the large volume rhyolites of the Snake River Plain is similar to that proposed by Frost and Frost (1997) and Streck and Grunder (2007). However, it is not universally accepted. For example, Boroughs et al. (2005) and Bonnicksen et al. (2007) propose that the rhyolitic magmas of the central Snake River Plain are largely derived by partial melting of “calc-alkaline” crustal rocks similar to the granitic rocks of the Idaho batholith. These contrasting proposals continue to frame the debate about the origin of A-type granitoids worldwide and show that we still have much to learn about these fascinating silicic magmas.

**Acknowledgments** We are grateful for collaboration with many people especially Myron Best and Scott Hughes. Reviews by Carol Frost and Michael Dorais were very helpful. This research has been funded by the National Science Foundation and the National Park Service.

## References

- Anderson L, Morrison J (2005) Ilmenite, magnetite, and peraluminous Mesoproterozoic anorogenic granites of Laurentia and Baltica. *Lithos* 80:45–60, DOI 10.1016/j.lithos.2004.05.008
- Armstrong RL, Leeman WP, Malde HE (1975) K–Ar dating, quaternary and Neogene volcanic rocks of the Snake River Plain, Idaho. *Am J Sci* 275:225–251
- Barr DL (1993) Time, space, and composition patterns of middle Cenozoic mafic to intermediate composition lava flows of the Great Basin, western USA. MS thesis, Brigham Young University, Provo, UT
- Best MG, Christiansen EH (1991) Limited extension during peak tertiary volcanism, Great Basin of Nevada and Utah. *J Geophys Res* 96:13509–13528
- Best MG, Christiansen EH (2001) *Igneous petrology*. Blackwell, Malden, MA
- Best MG, Christiansen EH, Blank HR (1989) Oligocene caldera complex and calc-alkaline tuffs and lavas of the Indian Peak volcanic field, Nevada and Utah. *Geol Soc Amer Bull* 101:1076–1090
- Best MG, Scott RB, Rowley PD, Swadley WC, Anderson RE, Grommé CS, Harding AE, Deino AL, Christiansen EH, Tingey DG, Sullivan KR (1993) Oligocene–Miocene caldera complexes, ash-flow sheets, and tectonism in the central and southeastern Great Basin. In: Lahren, MM, Trexler, JH, Jr (eds) *Crustal evolution of the Great Basin and the Sierra Nevada*. Geological Society of America Field Trip Guidebook, pp. 285–312
- Bindeman IN, Valley JW (2001) Low-delta  $^{18}O$  rhyolites from Yellowstone; magmatic evolution based on analyses of zircons and individual phenocrysts. *J Petrol* 42:1491–1517
- Bonin B (2005) A-type granites: Definitions, facts and speculations. *Goldschmidt Conference Abstracts 2005*, Moscow, Idaho
- Bonnicksen B (1982) Rhyolite lava flows in the Bruneau-Jarbridge eruptive center, southwestern Idaho. In: Bonnicksen B, Breckenridge RM (eds) *Cenozoic geology of Idaho: Idaho Bureau of Mines and Geol Bull* 26:282–320
- Bonnicksen B, Citron GP (1982) The Cougar Point Tuff, southwestern Idaho and vicinity. In: Bonnicksen B, Breckenridge RM (eds) *Cenozoic Geology of Idaho: Idaho Bureau of Mines and Geol Bull* 26:255–282
- Bonnicksen B, Leeman WP, Honjo N, McIntosh WC, Godchaux MM (2007) Miocene silicic volcanism in southwestern Idaho: geochronology, geochemistry, and evolution of the central Snake River Plain. *Bull Volcanol* (in press).
- Boroughs S, Wolff J, Bonnicksen B, Godchaux M, Larson P (2005) Large volume, low- $^{18}O$  rhyolites of the central Snake River Plain, Idaho, USA. *Geology* 33:821–824
- Carmichael ISE (1991) The redox states of basic and silicic magmas: a reflection of their source regions? *Contrib Mineral Petrol* 106:129–141
- Cathey HE, Nash BP (2004) The Cougar Point Tuff: implications for thermochemical zonation and longevity of high-temperature, large-volume silicic magmas of the Miocene Yellowstone hotspot. *J Petrol* 45:27–58
- Champion DE, Lanphere MA, Anderson SR, Kuntz MA (2002) Accumulation and subsidence of the Pleistocene basaltic lava flows of the eastern Snake River plain, Idaho. In: Link PK, Mink LL (eds) *Geology, hydrogeology, and environmental remediation*. *Geol Soc Am Special Paper*, vol. 353. Idaho National



- Engineering and Environmental Laboratory, Eastern Snake River Plain, Idaho, pp. 175–192
- Christiansen RL (2001) The Quaternary and Pliocene Yellowstone Plateau volcanic field of Wyoming, Idaho, and Montana, Geology of Yellowstone National Park. US Geol Surv Professional Paper 729
- Christiansen EH (2005a) Miocene magmatic transition in the northern Basin and Range province, western United States. Goldschmidt Conference Abstracts 2005, Moscow, Idaho
- Christiansen EH (2005b) Contrasting processes in silicic magma chambers: Evidence from very large volume ignimbrites. *Geol Mag* 142:669–681
- Christiansen EH, Hurst M (2004) Vent geology of low-shield volcanoes from the central Snake River Plain, Idaho. Lessons for Mars and the Moon: Lunar and Planetary Science Conference XXV, <http://www.lpi.usra.edu/meetings/lpsc2004/>
- Christiansen EH, Burt DM, Sheridan MF (1986) The geology of topaz rhyolites from the western United States. *Geol Soc Am Special Paper* 205:82
- Christiansen RL, Foulger GE, Evans JR (2002) Upper-mantle origin of the Yellowstone Hotspot. *Geol Soc Amer Bull* 114:1245–1256
- Chuang FC, McKee EH, Howard KA (2003) Hydrogeologic Factors that Influence Ground Water Movement in the Desert Southwest United States. US Geol Surv Open-File Report 38
- Collins WJ, Beams SD, White AJR, Chappell BA (1982) Nature and origin of A-type granites with particular reference to southeastern Australia. *Contrib Mineral Petrol* 80:189–200
- DePaolo DJ, Perry FV, Baldrige WS (1992) Crustal versus mantle sources of granitic magmas; a two-parameter model based on Nd isotopic studies. *Geol Soc Am Special Paper* 272:439–446
- Ekren EG, McIntyre DH, Bennet EH (1984) High temperature, large volume, lavalike ash-flow tuffs without calderas in southwestern Idaho. *US Geol Surv Professional Paper* 1272:73
- Ewart A (1979) A review of the mineralogy and chemistry of Tertiary-Recent dacitic, latitic, rhyolitic, and related salic volcanic rocks. Elsevier, Amsterdam, p 13–121
- Ewart A, Marsh JS, Milner SC, Duncan AR, Kamber BS, Armstrong RA (2004) Petrology and geochemistry of Early Cretaceous bimodal continental flood volcanism of the NW Etendeka, Namibia; Part 1, Introduction, mafic lavas and re-evaluation of mantle source components. *J Petrol* 45:59–105
- Frintd S, Haapala I, Pakkanen L (2004) Anorogenic Gross Spitzkoppe granite stock in central western Namibia; Part I, Petrology and geochemistry. *Am Mineral* 89:841–856
- Frost CD, Frost BR (1997) Reduced rapakivi-type granites: the tholeiite connection. *Geology* 25:647–650
- Frost BR, Barnes CG, Collins WJ, Arculus RJ, Ellis DJ, Frost CD (2001) A geochemical classification for granitic rocks. *J Petrol* 42:2033–2048
- Gill JB (1981) Orogenic andesites and plate tectonics. Springer, Berlin Heidelberg New York
- Greeley R (1982) The Snake River Plain, Idaho: representative of a new category of volcanism. *J Geophys Res* 87:2705–2712
- Hart GL (1997) An oxygen isotope investigation of the Indian Peak Volcanic Field, southern Utah–Nevada: magma source constraints for a late Oligocene caldera system. MS thesis, Brigham Young University, Provo, UT
- Hildreth W (1981) Gradients in silicic magma chamber; implications for lithospheric magmatism. *J Geophys Res* 86:10153–10192
- Hildreth W, Halliday AN, Christiansen RL (1991) Isotopic and chemical evidence concerning the genesis and contamination of basaltic and rhyolitic magma beneath the Yellowstone Plateau volcanic field. *J Petrol* 32:63–137
- Honjo N (1990) Geology and stratigraphy of the Mount Bennett Hills, and the origin of west-central Snake River Plain rhyolites. PhD thesis, Rice University, Houston, TX
- Honjo N, Leeman WP (1987) Origin of hybrid ferrolatite lavas from Magic Reservoir eruptive center, Snake River plain, Idaho. *Contrib Mineral Petrol* 96:163–177
- Honjo N, Bonnicksen B, Leeman WP, Stormer Jr JC (1992) Mineralogy and geothermometry of high-temperature rhyolites from the central and western Snake River plain. *Bull Volcanol* 54:220–237
- Hughes SS, McCurry M (2002) Bulk major and trace element evidence for a time-space evolution of Snake river Plain rhyolites, Idaho. In: Bonnicksen B, White CM, McCurry M (eds) Tectonic and magmatic evolution of the Snake River Plain volcanic province, vol. 30. Idaho Geological Survey Bulletin, pp. 161–176
- Kellogg KS, Harlan SS, Mehnert HH, Snee LW, Pierce KL, Hackett WR, Rodgers DW (1994) Major 10.2-Ma rhyolitic volcanism in the eastern Snake River plain, Idaho; isotopic age and stratigraphic setting of the Arbon Valley Tuff Member of the Starlight Formation. *US Geological Survey Bulletin*, vol. 2091
- Keppeler H (1996) Constraints from partitioning experiments on the composition of subduction zone fluids. *Nature* 380:237–240
- King PB, Beikman HM (1974) Geologic map of the United States (exclusive of Alaska and Hawaii). US Geological Survey, 1/250,000
- King PL, Chappell BW, Allen CM, White AJR (2001) Are A-type granites the high-temperature felsic granites? Evidence from fractionated granites of the Wangrah Suite. *Aust J Earth Sci* 48:501–514
- Leeman WP (1982) Rhyolites of the Snake River plain–Yellowstone Plateau Province, Idaho and Wyoming; a summary of petrogenetic models. In: Bonnicksen B, Breckenridge RM (eds) Cenozoic Geology of Idaho: Bull Idaho Bureau Mines Geol 26:203–212
- Leeman WP, Vitaliano CJ (1976) Petrology of McKinney Basalt, Snake River Plain, Idaho. *Geol Soc Amer Bull* 87:1777–1792
- Leeman WP, Vitaliano CJ, Prinz M (1976) Evolved lavas from the Snake River plain; craters of the Moon National Monument, Idaho. *Contrib Mineral Petrol* 56:35–60
- Leeman WP, Menzies MA, Matty DJ, Embree GF (1985) Strontium, neodymium, and lead isotopic compositions of deep crustal xenoliths from the Snake River Plain: Evidence for Archean basement. *Earth Planet Sci Lett* 75:354–368
- Mabey DR (1978) Regional gravity and magnetic anomalies in the eastern Snake River plain, Idaho. *J Res US Geol Surv* 6:553–562
- Manduca CA, Kuntz MA, Silver LT (1993) Emplacement and deformation history of the western margin of the Idaho Batholith near McCall, Idaho; influence of a major terrane boundary. *Geol Soc Amer Bull* 105:749–765
- Manley CR, McIntosh WC (2002) The Juniper Mountain Volcanic Center, Owyhee County, southwestern Idaho: age relations and physical volcanology. In: Bonnicksen B, White CM, McCurry M. (eds) Tectonic and magmatic evolution of the Snake River Plain Volcanic Province. Idaho Geological Survey Bull 30:205–227
- Marrett R, Emerman SH (1992) The relations between faulting and mafic magmatism in the Altiplano-Puna plateau (central Andes). *Earth Planet Sci Lett* 112:53–59
- Maughan L, Christiansen EH, Best MG, Gromme CS, Deino AL, Tingey DG (2001) The Oligocene Lund Tuff, Great Basin, USA: a very large volume monotonous intermediate. *J Volcanol Geotherm Res* 113:129–157
- McCurry M, Hackett WR, Hayden K (1999) Cedar Butte and cogenetic Quaternary rhyolite domes of the eastern Snake River Plain. In: Hughes SS, Thackray GD (eds) Guidebook to the geology of eastern Idaho. Idaho Museum of Natural History, pp 169–179
- McCurry M, Hayden K, Morse L (2007) Genesis of post-hotspot A-type rhyolite of the Eastern Snake River Plain volcanic province by extreme fractional crystallization of olivine tholeiite basalt: *Bull Volcanol* (in press)



- McDonough WF, Sun SS (1995) The composition of the earth. *Chem Geol* 120:223–253
- Miyashiro A (1974) Volcanic rock series in island arcs and active continental margins. *Am J Sci* 274:321–355
- Morgan WJ (1972) Plate motions and deep mantle convection. *Mem Geol Soc Amer* 132:7–22
- Nash BP, Perkins ME, Christensen JN, Lee D, Halliday AN (2006) The Yellowstone hotspot in space and time: Nd and Hf isotopes in silicic magmas. *Earth Planet Sci Lett* 247:143–156
- Nelson ST, Harris RA, Dorais MJ, Heizler M, Constenius KN, Barnett DE (2002) Basement complexes in the Wasatch Fault, Utah, provide new limits on crustal accretion. *Geology* 30:831–834
- Nielsen PJ (1992) Petrology of the Oligocene Shingle Pass Tuff in the Northern Basin and Range, Nevada: evolution of a dry, deduced magma system. MS thesis, Brigham Young University, Provo, UT
- Nusbaum RL (1990) Evidence for magma hybridization for the voluminous 29.5 Ma Wah Wah Springs Formation, Utah and Nevada, U.S.A. *J Volcanol Geotherm Res* 40:245–256
- Patiño Douce AE (1997) Generation of metaluminous A-type granites by low-pressure melting of calc-alkaline granitoids. *Geology* 25:743–746
- Pearce JA, Harris NB, Tindle AG (1984) Trace element discrimination diagrams for the tectonic interpretation of granitic rocks. *J Petrol* 25:956–983
- Peng X, Humphreys ED (1998) Crustal velocity structure across the eastern Snake River plain and the Yellowstone Swell. *J Geophys Res* 103:7171–7186
- Perkins ME, Nash WP (2002) Explosive silicic volcanism of the Yellowstone Hotspot; the ash fall tuff record. *Geol Soc Amer Bull* 114:367–381
- Perkins ME, Brown FH, Nash WP, McIntosh W, Williams SK (1998) Sequence, age, and source of silicic fallout tuffs in middle to late Miocene basins of the northern Basin and Range Province. *Geol Soc Amer Bull* 110:344–360
- Phillips LV (1989) The petrology and magmatic evolution of the large-volume ash-flow tuffs of the central Nevada caldera complex, Nye County, Nevada. PhD thesis, University of Georgia, Athens
- Pierce KL, Morgan LA (1992) The track of the Yellowstone hot spot; volcanism, faulting, and uplift. In: Link PK, Kuntz MA, Platt LB (eds) *Regional geology of eastern Idaho and western Wyoming*. *Mem Geol Soc Amer* 179:1–53
- Putirka KD, Mikaelian H, Ryerson F, Shaw H (2003) New clinopyroxene-liquid thermobarometers for mafic, evolved, and volatile-bearing lava composition, with applications to lavas from Tibet and the Snake River plain, Idaho. *Am Mineral* 88:1542–1554
- Radke LE, Best MG, Christiansen EH (1992) Petrology and temporal evolution of the rhyolite ash-flow tuffs of the 35.4 Ma Stone Cabin Formation, central Nevada. *Eos Trans AGU* 73:623
- Rämö OT, Haapala I (1995) One hundred years of rapakivi granite. *Mineral Petrol* 52:29–185
- Rapp RP, Watson EB (1995) Dehydration melting of metabasalt at 8–32 kbar; implications for continental growth and crust-mantle recycling. *J Petrol* 36:891–931
- Ross KT, Christiansen EH, Best MG, Dorais MJ, Tingey DG (2002) Petrology and emplacement of the Cottonwood Wash Tuff. *Geol Soc Am Abstracts with Programs* 34(3):9
- Rudnick RL, Fountain DM (1995) Nature and composition of the continental crust: a lower crust perspective. *Rev Geophys* 33:267–309
- Smith RB (2004) The Yellowstone Hotspot; plume or plum. *Abstracts with Programs Geol Soc Am* 36:96
- Smith RB, Braile LW (1994) The Yellowstone hotspot. *J Volcanol Geotherm Res* 61:121–187
- Spear DB (1979) The geology and volcanic history of the Big Southern Butte-East Butte area, eastern Snake River plain, Idaho. PhD thesis, State University of New York, Buffalo
- Sparlin MA, Braile LW, Smith RB (1982) Crustal structure of the eastern snake River Plain determined from ray trace modeling of seismic refraction data. *J Geophys Res* 87:2619–2633
- Spulber SD, Rutherford MJ (1983) The origin of rhyolite and plagiogranite in oceanic crust: an experimental study. *J Petrol* 24:1–25
- Stout MZ, Nicholls J (1977) Mineralogy and petrology of Quaternary lavas from the Snake River plain, Idaho. *Can J Earth Sci* 14:2140–2156
- Stout MZ, Nicholls J, Kuntz MA (1994) Petrological and mineralogical variations in 2500–2000 yr B.P. lava flows, craters of the moon lava field, Idaho. *J Petrol* 35:1681–1715
- Streck MJ, Grunder AL (2007) Phenocryst-poor rhyolites of bimodal, tholeiitic provinces: the Rattlesnake Tuff and implications for mush extraction models. *Bull Volcanol* (in press)
- Taylor SR, McLennan SM (1985) *The continental crust: its composition and evolution*. Blackwell, Cambridge
- Thompson RN (1975) Primary basalts and magma genesis; II, Snake River Plain, Idaho, USA. *Contrib Mineral Petrol* 52: 213–232
- Watson EB, Harrison TM (1983) Zircon saturation revisited; temperature and composition effects in a variety of crustal magma types. *Earth Planet Sci Lett* 64:295–304
- Whitaker ML, Nekvasil H, Lindsley DH (2007) Can crystallization of olivine tholeiite give rise to potassic rhyolites? An experimental investigation. *Bull Volcanol* (in press)
- Wolf MB, Wyllie PJ (1995) Liquid segregation parameters from amphibolite dehydration melting experiments. *J Geophys Res* 100:15,611–15,621
- Wolf DE, Leeman WP, Vervoort JD (2005) U–Pb zircon geochronology of crustal xenoliths confirms presence of Archean basement beneath the central and eastern Snake River plain. *Geol Soc Am Abstracts with Programs* 37:60
- Wright KE, McCurry M, Hughes SS (2002) Petrology and geochemistry of the Miocene Tuff of McMullen Creek, central Snake River Plain, Idaho. In: Bonnicksen B, White CM, McCurry M (eds) *Tectonic and magmatic evolution of the Snake River Plain volcanic province*. *Idaho Geol Surv Bull* 30:177–194
- Yuan H, Dueker K (2005) Teleseismic P-wave tomogram of the Yellowstone plume. *Geophys Res Lett* 32: L07304. DOI 10.1029/2004GL022056